C-Reactive protein and embolization during carotid artery stenting. A serological and morphological study

G. Faggioli[1*], S. Fittipaldi[1,2*], R. Pini[1], E. Beltrandi[3], R. Mauro[1], A. Freyrie[1], C. Rapezzi[4], A. Stella[1] and G. Pasquinelli[2]

[1]Department of Specialistic Surgery and Anaesthesiological Sciences, [2]Surgical Pathology and [3]Clinical Pathology, Department of Haematology, Oncology and Clinical Pathology and [4]Cardiology, Cardio-Thoraco-Vascular Department, Ospedale S. Orsola, University of Bologna, Bologna, Italy

*G. Faggioli and S. Fittipaldi equally contributed to the manuscript

Summary. Introduction. High-sensitivity C-Reactive Protein (hsCRP) levels are correlated with vulnerable carotid plaques, although their impact on the outcome of carotid revascularization is unknown. The aim of our study was to investigate the correlation between hsCRP and embolization during carotid artery stenting (CAS). Methods. Patients with symptomatic carotid stenosis were submitted to CAS with distal protection filters. Serum hsCRP was analysed prior to CAS and patients were divided into two groups: Class I, patients presenting hsCRP<5 mg/l and, Class II, patients presenting hsCRP≥5 mg/l. Plaques were categorised by ultrasound grey scale measurement as homogenous and dishomogenous. Afterwards CAS filters were analyzed microscopically and ultrastructurally to determine the type and the amount of debris present, based on percentage of surface involvement (SI) and pore occluded (PO) by embolic material. Results. Fourteen patients underwent uneventful CAS, with a mean hsCRP of 11.5±18.4 mg/l. Eight patients were in Class I and six in Class II. All filters had microscopic debris. SI was 25.4% in Class I and 33.3% in Class II (p=ns), PO 22.9% and 33.3% respectively (p=0.049). Patients in Class II who also had a dishomogenous plaque showed greater SI and PO compared with patients in Class I with homogenous plaque (35.0% vs. 21.8% and 40.4% vs. 22.7% respectively, p<0.05). Microscopically embolic material was identified as atherosclerotic plaque fragments and platelet aggregates and was similar in both groups. Discussion. High hsCRP levels are associated with significantly greater embolization during CAS in symptomatic patients, particularly in dishomogenous plaque. Although these results need further investigation due to the limited number of enrolled patients, this study suggests that CAS may not be indicated as a method of carotid revascularization in this setting.

Key words: hsCRP, Filter stent, Inflammation, Vulnerable carotid plaque

Introduction

Inflammation is a key issue in atherosclerosis development since inflammatory mediators promote both subintimal cholesterol deposits and leukocyte recruitment (Ross, 1999). One of the most important of these mediators is C-Reactive Protein (CRP), which plays a direct pathogenic role by promoting inflammation through metalloproteinase and macrophage activation (Pasceri et al., 2000; Jialal et al., 2004; Venugopal et al., 2005; Montero et al., 2006; Tron et al., 2008).

High-sensitivity C-Reactive Protein (hsCRP) is also a marker for carotid atherosclerosis; its levels are related to the presence of macrophages and T lymphocytes in atherosclerotic lesions associated with plaque instability (Garcia et al., 2003; Krupinski et al., 2006; Albuquerque et al., 2007; Mullenix et al., 2007).

HsCRP could have a clinical relevance in carotid disease: elevated hsCRP levels predict the progression of carotid narrowing (Hashimoto et al., 2001; Schillinger et al., 2005; Arthurs et al., 2008) and symptomatic carotid plaques have higher hsCRP levels compared to

asymptomatic ones; high levels of hsCRP could therefore predict carotid atherosclerotic plaque instability and subsequent embolism (Rost et al., 2001; Rerkasem et al., 2002; Papas et al., 2008). In fact, the relationship between high hsCRP levels indicative of plaque instability and the outcome of endovascular procedures is well investigated in coronary artery disease (Dirk et al., 2001). The same relationship in the carotid territory has been scarcely investigated, even if plaque instability is an important risk factor for cerebral embolism in carotid artery stenting (CAS). Previous studies analysed debris captured by distal filter, showing the relationship between plaque structure and the amount of particles captured by the filter (Angelini et al., 2002; Quan et al., 2005; DeRubertis et al., 2007; Divani et al., 2008; Hayashi et al., 2009; Piñero et al., 2009).

The aim of the present study was to investigate the role of serum hsCRP as a marker of risk of plaque embolization during CAS, evaluating by light (LM) and scanning electron microscopy (SEM) the amount and type of embolic debris captured by distal filter.

Materials and methods

Patients

In the period between June 2009 and December 2009 a series of consecutive patients with ≥70% carotid artery stenosis (North American Symptomatic Carotid Endarterectomy Trial Collaborators, 1991) were submitted to CAS, according to Society for Vascular Surgery recommendations (Hobson et al., 2008). Demographic data, symptoms (amaurosis fugax, transient ischemic attack, minor and major stroke), vascular risk factors (hypertension, coronary artery disease, chronic obstructive pulmonary disease, dyslipidemia, diabetes mellitus, current smoking, chronic renal failure based on a glomerular filtration rate <60 ml/min) and current therapy (acetylsalicylic acid, anticoagulant, hydroxymethyl glutaryl coenzyme A reductase inhibitor) were all recorded in a database software. All patients gave the appropriate informed consent for the study before the CAS procedure.

Carotid plaque structure analysis

Carotid plaques were evaluated by duplex scan ultrasound (Philips, IU 22) to determine the role of plaque structure in CAS embolization; the images were digitally stored for later evaluation by an expert operator blinded to the study. The plaques were divided into homogeneous and dishomogeneous, according to gray scale measurement (GSM). GSM was analysed for each plaque with the ImageJ software (http://rsbweb.nih.gov/ij/) using the histogram function that gives a mean gray of pixels of the region of interest (Fig. 1). Dishomogeneous plaques were identified with GSM<50 (Biasi et al., 1999), or in the presence of an ulceration (defined as a surface recess greater than 2 mm deep and 2 mm long).

Measurement of circulating hsCRP

Serum hsCRP measurements were used as a surrogate marker of plaque embolic potential. Blood samples were collected 24 hrs prior to CAS and centrifuged at 1800 rpm for 10 min at room temperature (RT). Serum hsCRP levels were analysed through nephelometric analysis (Image, Beckman Instrument); following hsCRP determination patients were divided
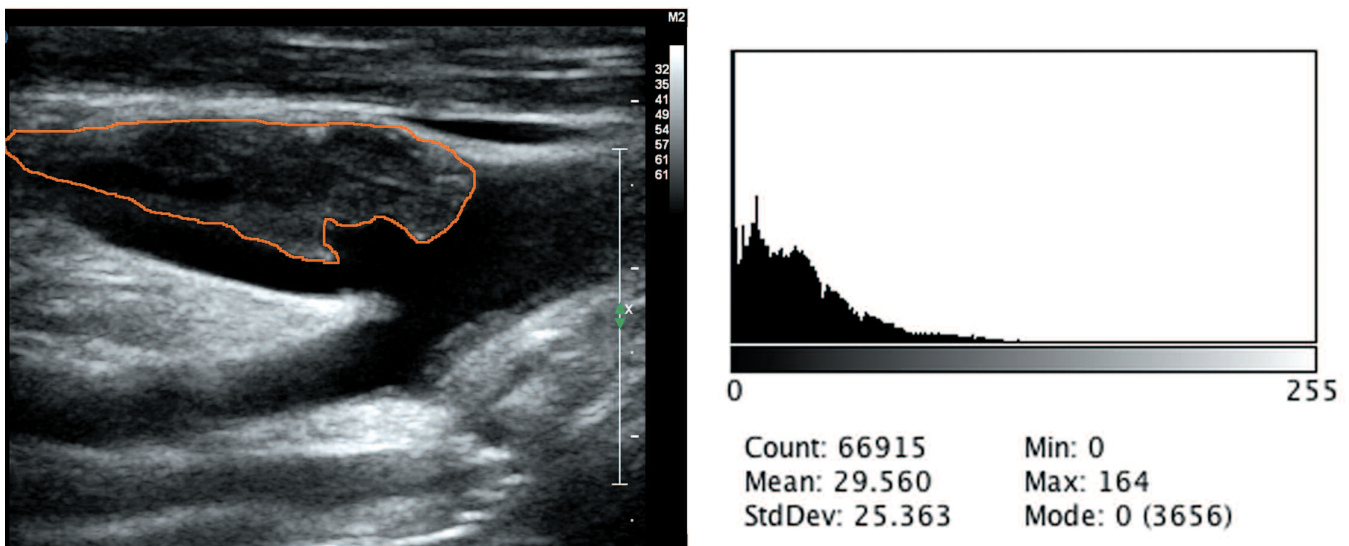

Fig. 1. Outline analysis of Grey Scale Measurement in the region of interest by ImageJ software. Identification of a dishomogeneous plaque according to the mean value of pixels gray (mean GSM< 50).

into two groups: Class I, hsCRP<5 mg/l and Class II, hsCRP≥5 mg/l. The threshold of 5 mg/l was chosen because higher serum hsCRP levels (≥5 mg/l) were previously associated with vulnerable inflammatory plaque at histological evaluation (Garcia et al., 2003) and with complication risk during CAS (Gröschnel et al., 2007).

CAS procedure

CAS was performed as previously described (Faggioli et al., 2007). Briefly, patients were taken to the angiographic suite after cardiological evaluation and medicated with aspirin 100 mg and clopidogrel 75 mg for 3 days before the procedure. All procedures were performed under local anaesthesia, systemic heparinisation and an 8F groin introducer. Common carotid cannulation was achieved with 40°C Boston Scientific® or Medtronic® HS I and II catheters over a Terumo® stiff guide wire. When cannulation was not achievable by these means, several different alternative techniques were used (i.e., buddy wire, coaxial). Brachial or carotid access was not attempted in any case. Routine cerebral protection was performed using Filterwire EZ with 100 μm diameter pores (Boston Scientific®) and stenting by closed-cell (Wallstent, Boston Scientific®). 'Technical success' was defined as the ability to treat the stenosis with less than 30% residual stenosis. Neurological outcome was evaluated both at the end of the procedure and in the following 24 h by a neurologist according to the NIH stroke scale and the modified Rankin scale.

Filter analysis by light microscopy

At the end of the CAS procedure filters were recovered, gently washed in physiological solution and immediately fixed in 10% neutral, buffered pH 6.9 formalin. Macro photographs of the device in its integrity were taken under a stereomicroscope. After removal of the metallic wire, the filter was cut into two equal portions and flattened; the first sample was mounted onto glass slides using Canada Balsam (Sigma-Aldrich C1795) whereas the second one was stored in formalin for SEM examination. Morphometric analysis was performed under a light microscope (Leitz Wetzlak, Germany) connected with a CCD camera Olympus CX42. Images were acquired using Image-Pro Plus software (Media Cybernetics) and processed with ImageJ software (http://rsbweb.nih.gov/ij/). An average of 30 fields per filter was acquired and the total area evaluated for each filter was 0.12 mm^2 at a magnification of x10.

The percentage of membrane surface occupied by debris was expressed as percentage of surface involvement (SI). Images were converted to stacks composed by 6 fields each, transformed in montage, converted from colour images to 8-bit greyscale with the scale set at 0.41 pixel/μm. The boundary of the filters was delineated to calculate the total area for each stack (13.2mm^2), and then the lower and upper threshold values were set to measure the percentage of the covered area of interest (Fig. 2A,B).

The number of pores occluded (PO) by thrombo-embolic material, with a minimum mean size of 40 μm, and the total number of non-occluded pores was quantified and expressed as a percentage (Fig. 2C,D). For histology and debris characterisation, the apex of some filters with visible adherent material was recovered, dehydrated as before and embedded in paraffin for 1h; 3 μm thick sections were stained with hematoxylin-eosin (HE).

Filter analysis by scanning electron microscopy

Scanning electron microscopy (SEM) was performed to characterize the dimension and the type of embolic debris adherent to the filter device inner surface.

Filters were embedded in ashless paper filters, washed with phosphate buffer 0.15 M and post-fixed in 1% osmium tetroxide for 15 min at RT. Then the filters were washed for 15 min in distilled water, dehydrated with graded steps of ethanol (70%, 95% and 100% ethanol; 15 min each step) and dried with hexamethyldisilazene (HMDS, Fluka, Steinheim, Germany) for 30 min at RT. The dried filters were accurately flattened and mounted on aluminium stubs (Multilab Type stub pin 1/2'', Surrey, UK), and sputter coated with a 10 nm thick layer of gold in a Balzers MED 010 sputtering device (Balzer Union FL 9496 Furstenstum, Liechtenstein). Then samples were observed using a Philips 505 Scanning Electron Microscope at 15 kV. Images were processed with ImageJ. The size of the particles was evaluated by measuring the length of major and minor axis using ImageJ.

Statistical analysis

Quantitative variables were expressed as a mean ± standard deviation (SD), qualitative variables by relative and absolute frequencies. Analysis of differences between Class I and Class II were performed with Fisher's test for qualitative variables and with Student's t-test for quantitative variables. One-Way ANOVA test and post-hoc analysis were performed to evaluate significant differences for average PO and SI between more than two groups. P value <.05 was considered statistically significant. Statistical tests were performed using SPSS® 13.0 for Windows® computer software (SPSS, Chicago, Illinois, USA).

Results

Patients

Sixteen patients were included in the study. In fourteen patients the procedure was achieved

successfully. In two cases the CAS procedure was aborted due to technical difficulties and the stent was not deployed. However in both these cases the filter was positioned and subsequently removed and was utilized as a control specimen.

Mean hsCRP was 11.5±18.4 mg/l (range 0.21-67.8 mg/l), 8 patients were in Class I with a mean hsCRP 1.9±1.4 mg/l, 6 patients were in Class II with a mean hsCRP 24.2±23.3 mg/l. No significant differences were found in demographic data, symptoms, vascular risk factors and current therapy of the two groups and the data are summarised in Table 1.

Drug therapy

Anticoagulant therapy was not used by patients enrolled in the present study. Antiaggregant therapy prior the enrollment was used by 14 patients, 8 in Class I and 6 in Class II (p=ns). As described in CAS procedure, all patients were medicated with aspirin 100 mg and clopidogrel 75 mg for 3 days before and one month after the procedure. Hydroxymethyl glutaryl-coenzyme A-
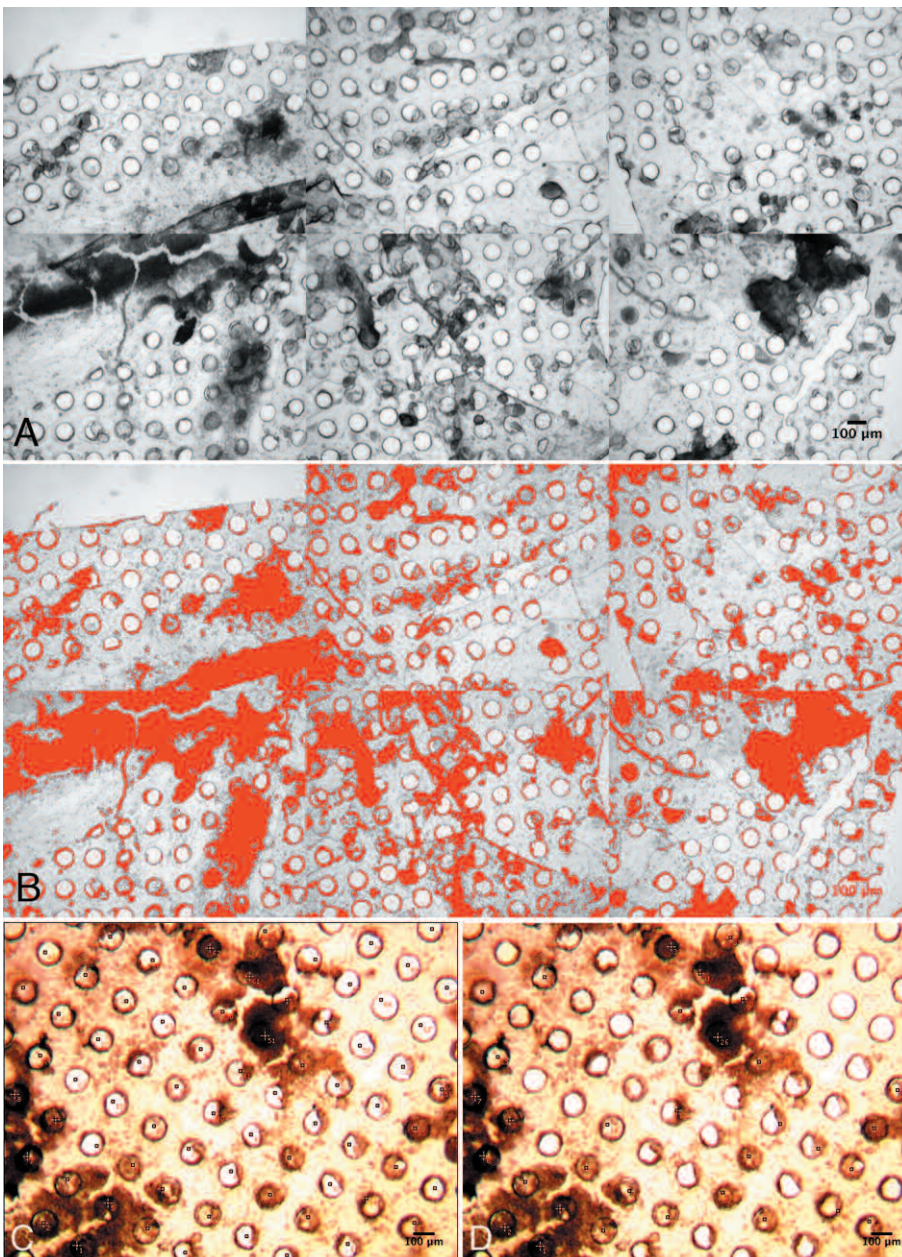

Fig. 2. Filter membrane showing the evaluation of the covered area by embolic debris at light microscopy; surface involvement (SI) = 25.1% (**A, B**); counting of occluded pores (PO) = 46,4% (**C, D**). Scale bar: 100 μm.

reductase inhibitor (statins) therapy was used by 6 patients, 4 (50%) in Class I and 2 (33%) in Class II (p=ns). No significant difference was seen in filter PO, SI and SEM evaluation between patients with or without statins therapy (data not shown).

Filter analysis by light microscopy

All filters showed the presence of a substantial amount of debris at macroscopic observation. Two of them had extensive deposits of vitreous, yellowish lipid-like material that was dissolved after histological processing (Fig. 3). Microscopic debris were detected in all filters, with a percentage of surface involvement (SI) of 28.8±8.1% and pore occluded (PO) of 27.3±9.5%; control filters showed both a lower SI, 4.15±2.3%, and PO, 0.5±0.3%, compared to filters of treated patients (p<0.05). Class II had a greater percentage of PO and a trend towards greater percentage of SI compared with Class I (35.7±11.7% vs. 23.9±6.7%, p=0.049 and 33.3±7.7% vs. 25.4±7.0%, p=0.07 respectively) (Fig. 4A,B).

According to the type of plaques, patients (n.6) with dishomogeneous plaque had a significantly higher SI vs those with homogeneous plaque (n.8) (33.9±7.1% vs. 23.7±5.6% respectively, p=0.01), and a trend towards greater PO (34.2±11.8% vs 23.8±6.7%, p=0.07). Class II patients with dishomogeneous plaque had significantly

Table 2. Mean size of the debris adherent to the inner membrane of the filter.

	Mean-size-(MA) μm	SD
Embolus	161	±128
Biofilm	713	±398
Thromboembolic material	876	±689
Plaque fragment	1419	±650

MA: Major axis; SD: standard deviation.

Table 1. Characteristics of the study population.

Characteristics*	Class I	Class II	P value
Age, years	77.0±5.3	72.3±11.3	Ns
Male gender	62% (5)	100% (6)	Ns
Vascular risk factors			
Hypertension	100% (8)	100% (6)	Ns
Coronary-artery disease	75% (6)	66% (4)	Ns
Chronic-obstructive pulmonary disease	12% (1)	66% (4)	Ns
Dyslipidemia	62% (5)	50% (3)	Ns
Current smoking	12% (1)	0% (0)	Ns
Chronic-renal failure (GFR < 60 ml/min)	12% (1)	50% (3)	Ns
Symptoms			
Amaurosis fugax	12% (1)	0% (0)	Ns
TIA	37% (3)	33% (2)	Ns
Minor-and-major stroke	25% (2)	33% (2)	Ns
Current therapy			
ASA	100% (8)	100% (6)	Ns
Anticoagulant	0% (0)	0% (0)	Ns
Hydroxymethyl glutaryl-coenzyme A-reductase inhibitor	50% (4)	33% (2)	Ns

ASA: acetylsalicylic acid; TIA: Transient Ischemic Attack; ns: not significant; GFR: Glomerular filtration rate. *: Continous data are represented as mean SD.
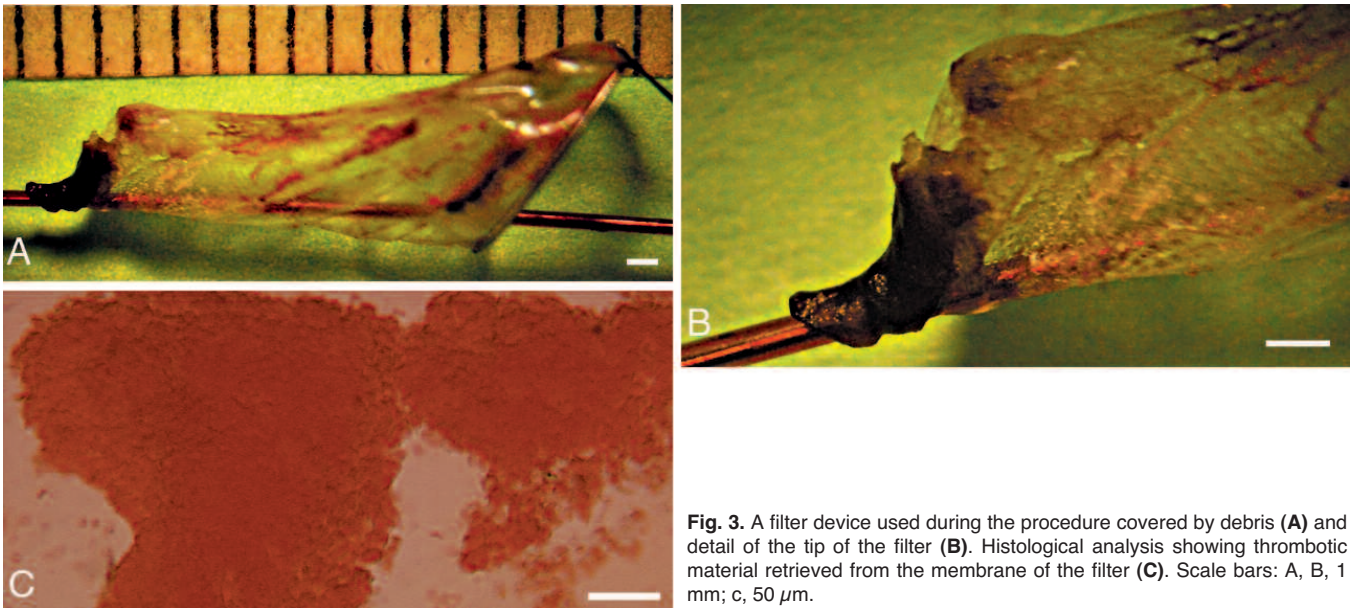

Fig. 3. A filter device used during the procedure covered by debris **(A)** and detail of the tip of the filter **(B)**. Histological analysis showing thrombotic material retrieved from the membrane of the filter **(C)**. Scale bars: A, B, 1 mm; c, 50 μm.

greater SI and PO compared to class I patients with homogeneous plaque (35.7±8.7% vs. 21.8±5.6% p=0.04 and 40.4±10.0% versus 22.7±6.8% p=0.04, respectively) (Fig. 4C,D).

Filter analysis by scanning electron microscopy

To further clarify the composition and the mean size of debris adherent to the inner surface part of the filter, devices were analysed through SEM and histological analysis. Unlike control filters, visibly clean (Fig. 5A), all areas of the filter were covered with debris ranging from 30 μm to 2 mm (Fig. 5B, Table 2). Distribution of the material was heterogeneous along the filter membrane with a significantly higher SI (37±9%) at the

tip of the filter (zone A) compared to the middle zone (zone B; 28±7.7%) and distal zone (zone C; 23±8.3%) (Fig. 6C). Plaque fragments were commonly seen at the tip of the filter (Fig. 6A,B). Hematoxylin-eosin staining revealed that the type of material removed from the paraffin embedded filters was composed by thrombo-embolic debris, acellular material, cholesterol clefts and atheromatous plaque fragments (Fig. 7).

All filters were covered with an amorphous film, i.e., biofilm, of protein composition typical for all biomaterial. Pores of 100 μm diameter were occluded by clumps of red blood cells (RBC), embolic and plaque fragments (Fig. 8). SEM also revealed the presence of activated platelets with dendritic and spread morphologies (Fig. 9).
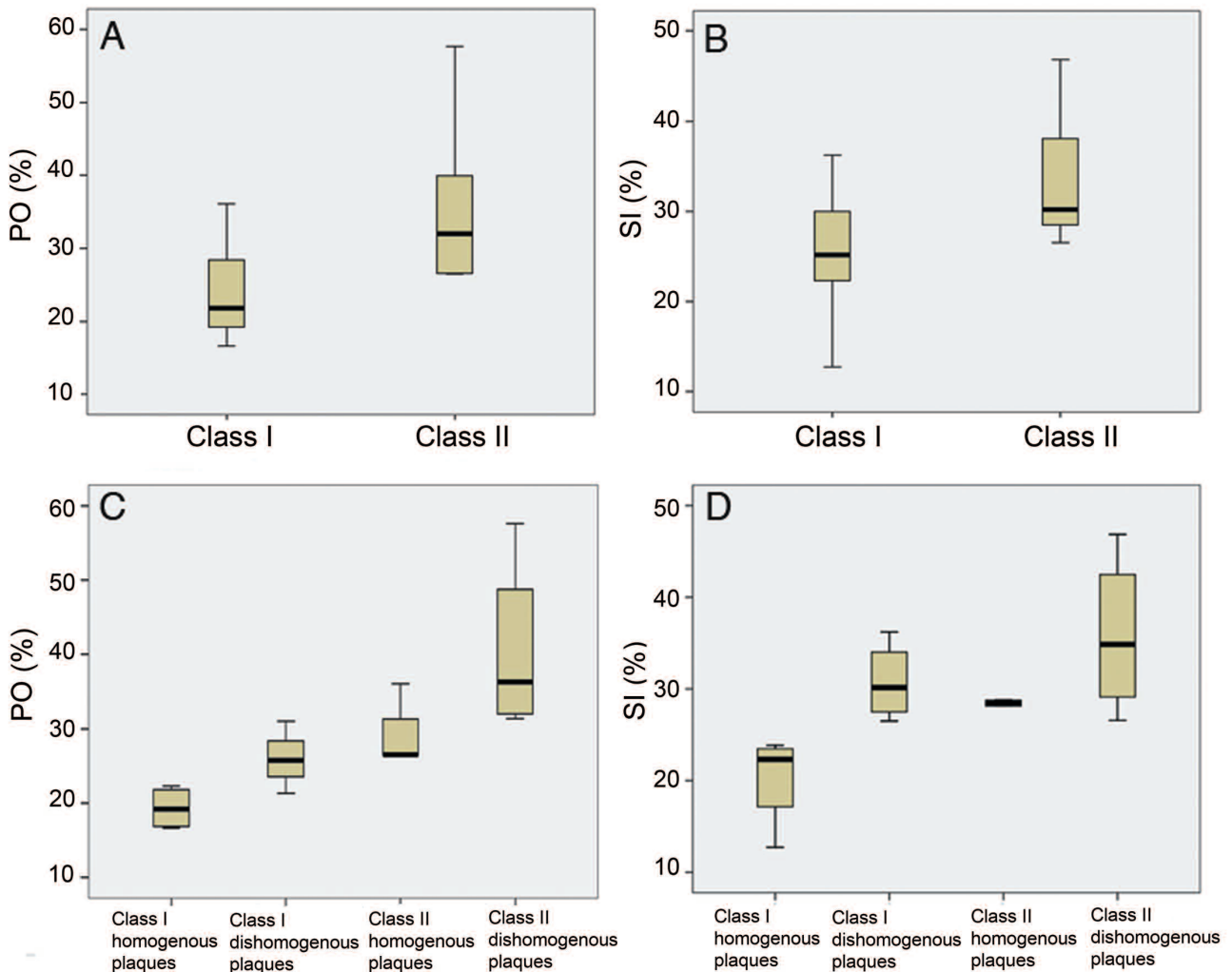

Fig. 4. Percentage of PO **(A)** and SI **(B)** in class I (hsCRP<5mg/l) and class II (hsCRP>5mg/l) patients. Differences between percentage of PO **(C)** and SI **(D)** in patients within class I with homogenous or dishomogenous plaque and patients within class II with homogenous or dishomogenous plaque.

No differences were found in volume and composition of embolic debris between class I and class II or in patients with homogeneous and dishomogeneous plaque (data not shown).

Discussion

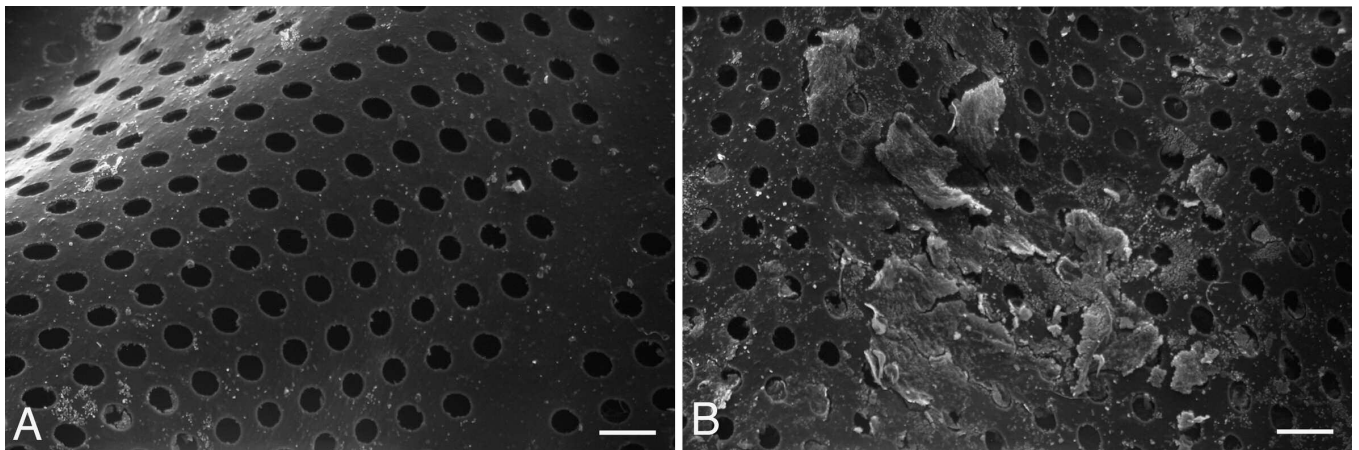The risk of embolization from carotid plaque is of paramount importance both in indication to

Fig. 5. Scanning electron microscopy image of the luminal surface of the control filter membrane **(A)** and a filter used during CAS containing adherent debris and visibly occluded pores **(B)** with a diameter of 100 μm. Scale bar: 200 μm.
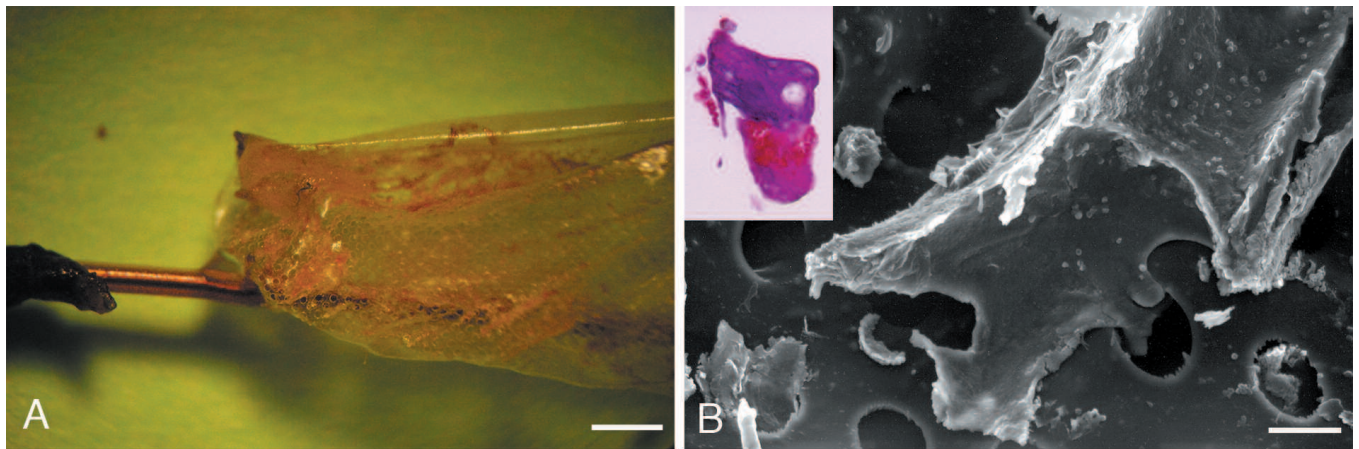

Fig. 6. A filter used during CAS **(A)** and the corresponding scanning electron microscopy showing details of the point with accumulation of embolic material **(B)**. Hematoxylin-eosin staining of a plaque fragment removed from the filter point **(B, insert)**. Distribution of embolic material (% SI) in three different zones of the filter: distal (zone C), medial (zone B) and proximal (zone A). Scale bars: A, 1 mm; B, 100 μm. Insert in B, x 40
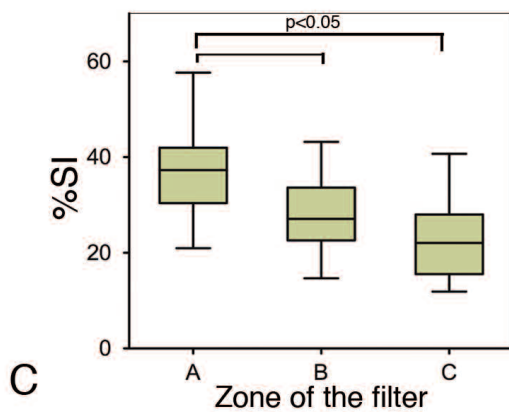
revascularization and during the carotid endovascular procedure. However, methods to objectively identify this risk are not presently available. Several methods have been suggested, (i.e. GSM, Magnetic Resonance imaging, Computed Tomography, etc.) although no study has correlated the amount of embolic debris in CAS procedure and serological markers such as CRP. In this study we examined filters obtained by the CAS procedure, with the intention of evaluating the amount and the pattern of filter involvement by emboli, indicative of the vulnerability of the plaque treated.

The first important finding was that all filters showed a certain amount of emboli, confirming previous data showing the high embolic potential of the CAS procedure. Previous studies showed a high rate of

asymptomatic cerebral lesions during CAS with Diffusion-Weight Magnetic Resonance Imaging (Poppert et al., 2004; Roh et al., 2005; Faggioli et al., 2009; Lacroix et al., 2009; Skjelland et al., 2009). According to our data, not all plaques behave similarly; patients with CRP above 5 mg/l (Class II) showed a significantly increased number of pores occluded, indicative of debris greater than the size of pore filter, i.e., 100 μm.

A second finding of the present study was a trend towards greater filter surface involvement in Class II patients; however one should consider that this analysis might be influenced by deposition of the protein biofilm commonly seen in all implanted materials. Moreover, the filter surface was focally covered with activated
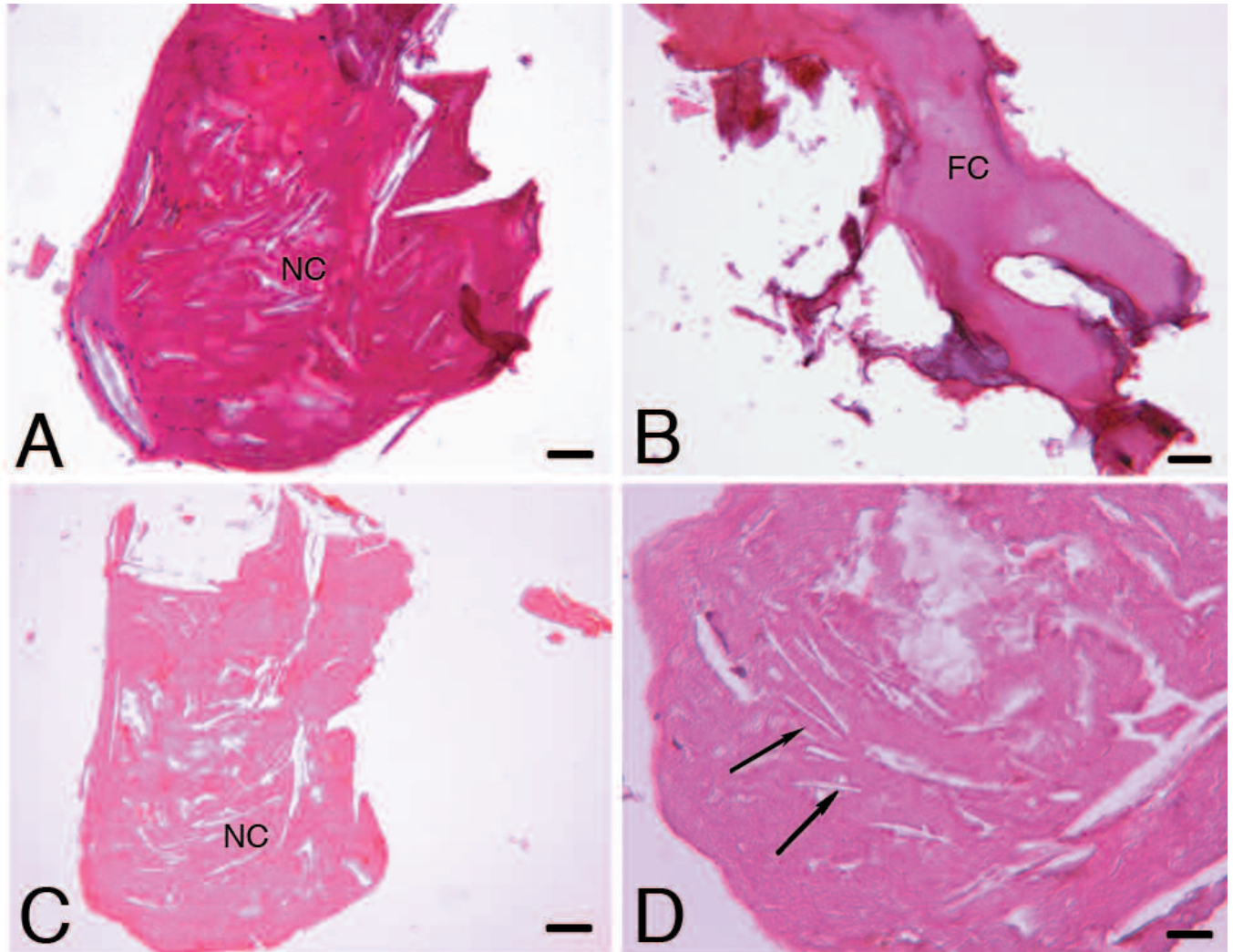

Fig. 7. Histological images of debris recovered from the entire filter membrane showing necrotic-lipid core **(A and C**; FC) and fibrous cap **(B**; NC) fragments; **D)** higher magnification of panel **C** showing amorphous and acellular material rich in cholesterol clefts (arrows). Scale bars: A, B, C, 100 μm; D, 5 μm.
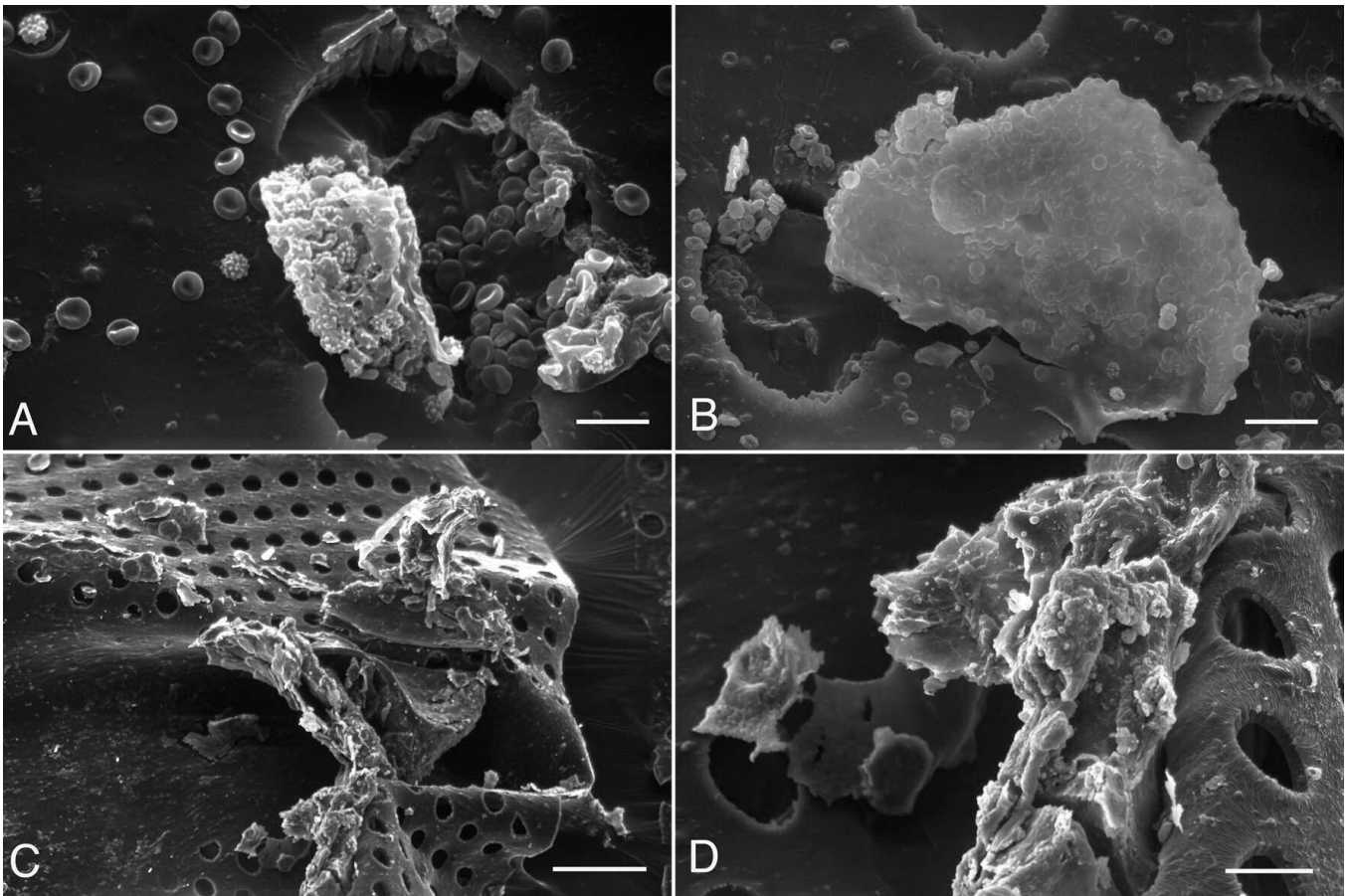
Fig. 8. Representative scanning electron microscopic images of thromboembolic materials captured by the filter surface **(A and B)**. Details of plaque fragment trapped at the filter's tip **(C and D)**. Scale bars: A, 25 µm; B, 40 µm; C, 500 µm; D, 100 µm.
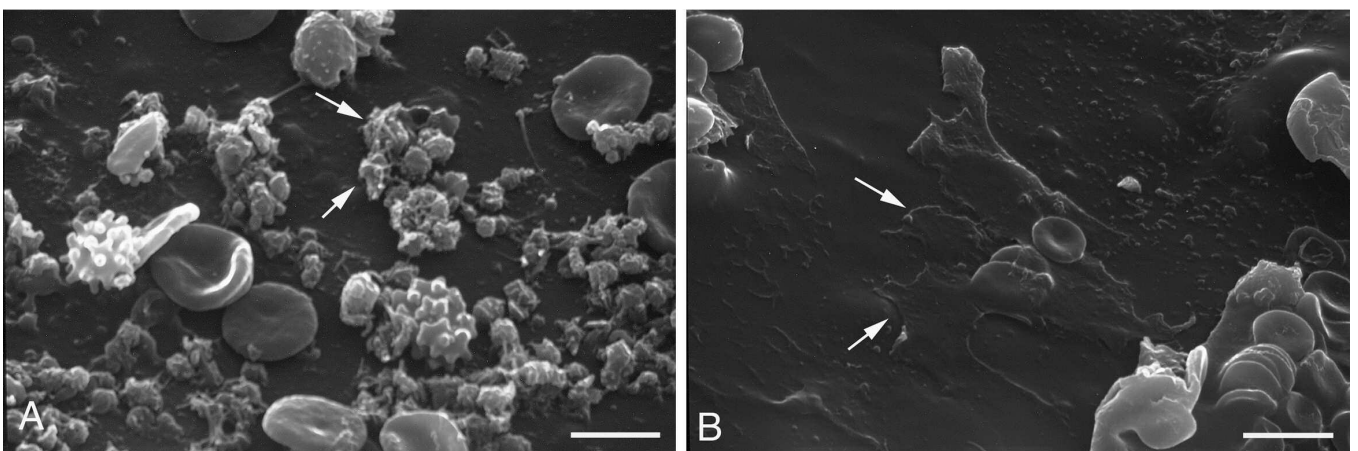

Fig. 9. Surface filter showing a variety of cells ranging from red blood cells, acanthocytes, aggregates of dendritic, activated platelets (white arrows; **A**) and fully spread platelets (white arrows; **B**). Scale bars: A, 5 µm; B, 10 µm.

platelets, a feature suggesting a certain degree of material thrombogenicity.

These findings and their correlation with the embolic potential of the plaque is supported by the relationship existing with echographic characteristics of the plaques: dishomogenous plaques showed a significantly greater percentage of both PO and SI, which further supports the clinical findings of their higher embolic potential. In this sense, it is not surprising that patients with elevated CRP (Class II) and dishomogenous plaque had an even greater percentage of PO.

Ultrastructural appearance of the debris and histological analysis showed features consistent with the plaque origin of the emboli; it should be outlined that in the CAS technique employed in this study, filters are opened only during stent deployment and dilatation. We can therefore reasonably exclude other possible origins of embolic material, as confirmed by the analysis of the control filters. Moreover, the amorphous material retrieved from the filter membrane originated from dislocated fragments of the necrotic core during the procedure. These results confirm the data obtained in previous studies evaluating the nature of embolic debris captured during the procedure (Angelini et al., 2002; Hayashi et al., 2009).

Angelini et al. (2002), previously described the embolic materials seen in the cerebral protection filter after CAS but did not attempt any clinical or serological association with the amount of captured emboli. Gröschnel et al., 2007 reported a correlation with high hsCRP levels (≥ 5 mg/l) and the incidence of adverse events in CAS, speculating that inflammation may be related. In the present study high hsCRP levels (≥ 5 mg/l) are correlated with the amount of embolic material seen in cerebral filters, demonstrating the relationship between carotid plaque structure, inflammation and the embolic potential in CAS.

The major limitation of the present study is the low number of the enrolled patients; however, our results suggest hsCRP serum evaluation may have a useful role for identification of vulnerable atherosclerotic plaque and for minimizing the subsequent risk in endovascular procedures.

To consolidate these data, larger numbers of patients are required. Currently new data regarding the quantification of cerebral lesions post procedural were obtained based on diffusion weight magnetic resonance imaging. Preliminary data suggest the higher incidence of cerebral micro-embolization during CAS in patients with a higher percentage of SI and in class II patients (data unpublished). Thus, the amount of debris on the filter and the level of hsCRP are associated with an increased embolization; this would be crucial in setting indication to carotid revascularization procedures.

Limitation of the study: relatively low number of cases examined, reducing the statistical power of subgroup analysis. The lack of cerebral imaging indicative of embolization during CAS reduces the technical implication of the study.

References

Albuquerque L.C., Narvaes L.B., Maciel A.A., Staub H., Friedrich M., Filho J.R., Marques M.B. and Rohde L.E. (2007). Intraplaque hemorrhage assessed by high-resolution magnetic resonance imaging and C-reactive protein in carotid atherosclerosis. J. Vasc. Surg. 46, 1130-1137.

Angelini A., Reimers B., Della Barbera M., Saccà S., Pasquetto G., Cernetti C., Valente M., Pascotto P. and Thiene G. (2002). Cerebral protection during carotid artery stenting. Collection and histopathologic analysis of embolized debris. Stroke 33, 456-461.

Arthurs Z.M., Andersen C., Starnes B.W., Sohn V.Y., Mullenix P.S. and Perry J. (2008). Prospective evaluation of C-reactive protein in the progression of carotid artery stenosis. J. Vasc. Surg. 47, 744-751.

Biasi G.M., Sampaolo A., Mingazzini P., De Amicis P., El-Barghouty N. and Nicolaides A.N. (1999). Computer analysis of ultrasonic plaque echolucency in identifying high risk carotid bifurcation lesions. Eur. J. Vasc. Endovasc. Surg. 17, 476-479.

DeRubertis B.G., Chaer R.A., Gordon R., Bell H., Hynecek R.L., Pieracci F.M., Karwowski J., Kent K.C. and Faries PL. (2007). Determining the quantity and character of carotid artery embolic debris by electron microscopy and energy dispersive spectroscopy. J. Vasc. Surg. 45, 716-724.

Divani A.A., Berezina T.L., Zhou J., Pakdaman R., Suri M.F. and Qureshi A.I. (2008). AI.Microscopic and macroscopic evaluation of emboli captured during angioplasty and stent procedures in extracranial vertebral and internal carotid arteries. J. Endovasc. Ther. 15, 263-269.

Dirk H.W., Stephan F., Sellwig M., Auch-Schwelk W., Schächinger V. and Zeiher A.M. (2001). Preprocedural C-reactive protein levels and cardiovascular events after coronary stent implantation. J. Am. Coll. Cardiol. 37, 839-846.

Faggioli G.L., Ferri M., Gargiulo M., Fratesi F., Manzoli L. and Stella A. (2007). Measurement and impact of proximal and distal tortuosity in carotid stenting procedures. J. Vasc. Surg. 46, 1119-1124.

Faggioli G.L., Ferri M., Serra C., Biagini E., Manzoli L., Lodi R., Rapezzi C. and Stella A. (2009). The Residual Risk of Cerebral Embolism after Carotid Stenting: The Complex Interplay between Stent Coverage and Aortic Arch Atherosclerosis. Eur. J. Vasc. Endovasc Surg. 37, 519-524.

Garcia B.A., Ruiz C., Chacon P., Sabin J.A. and Matas M. (2003). High-sensitivity C-reactive protein in high-grade carotid stenosis: Risk marker for unstable carotid plaque. J. Vasc Surg. 38, 1018-1024.

Gröschel K., Ernemann U., Larsen J., Knauth M., Schmidt F., Artschwager J. and Kastrup A. (2007). Preprocedural C-Reactive Protein Levels Predict Stroke and Death in Patients Undergoing Carotid Stenting. Am. J. Neuroradiol. 28, 1743-1746.

Hashimoto H., Kitagawa K., Hougaku H., Shimizu Y., Sakaguchi M., Nagai Y., Iyama S., Yamanishi H., Matsumoto M. and Hori M. (2001). C-reactive protein is an independent predictor of the rate of increase in early carotid atherosclerosis. Circulation 104, 63-67.

Hayashi K., Kitagawa N., Morikawa M., Hiu T., Morofuji Y., Suyama K. and Nagata I. (2009). Observation of the embolus protection filter for carotid artery stenting. Surg. Neurol. 72, 532-537

Hobson R.W., Mackey W.C., Ascher E., Murad M.H., Calligaro K.D., Comerota A.J., Montori V.M., Eskandari M.K., Massop D.W., Bush R.L., Lal B.K. and Perler B.A. (2008). Management of atherosclerotic carotid artery disease: Clinical practice guidelines of the Society for Vascular Surgery. J. Vasc Surg. 48, 480-486.

Jialal I., Devaraj S. and Venugopal S.K. (2004). C-Reactive Protein: Risk Marker or Mediator in Atherothrombosis? Hypertension 44, 6-11.

Krupinski J., Turu M.M., Martinez-Gonzalez J., Carvajal A., Juan-Babot J.O., Iborra E., Slevin M., Rubio F. and Badimon L. (2006). Endogenous expression of C-reactive protein is increased in active (ulcerated noncomplicated) human carotid artery plaques. Stroke. 37, 1200-1204.

Lacroix V., Hammer F., Astarci P., Duprez T., Grandin C., Cosnard G., Peeters A. and Verhelst R. (2007). Ischemic cerebral lesions after carotid surgery and carotid stenting. Eur. J. Vasc. Endovasc. Surg. 33, 430-435.

Montero I., Orbe J., Varo N., Beloqui O., Monreal J.I., Rodríguez J.A., Díez J., Libby P. and Páramo J.A. (2006). C-reactive protein induces matrix metalloproteinase-1 and -10 in human endothelial cells implications for clinical and subclinical atherosclerosis. J. Am. Coll. Cardiol. 47, 1369-78.

Mullenix P.S., Steele S.R., Martin M.J., Starnes B.W. and Andersen C.A. (2007). C-reactive protein level and traditional vascular risk factors in the prediction of carotid stenosis. Arch. Surg. 142, 1066-1071.

North American Symptomatic Carotid Endarterectomy Trial Collaborators. (1991). Beneficial effect of carotid endarterectomy in symptomatic patients with high-grade carotid stenosis. N. Engl. J. Med. 325, 445-453.

Papas T.T., Maltezos C.K., Papanas N., Kopadis G., Marakis J., Maltezos E. and Bastounis E. (2008). High-sensitivity CRP is correlated with neurologic symptoms and plaque instability in patients with severe stenosis of the carotid bifurcation. Vasc. Endovascular Surg. 42, 249-257.

Pasceri V., Willerson J.T. and Yeh E.T. (2000). Direct proinflammatory effect of C-reactive protein on human endothelial cells. Circulation 102, 2165-2168.

Piñero P., González A., Martínez E., Mayol A., Rafel E., González-Marcos J.R., Moniche F., Cayuela A. and Gil-Peralta A. (2009). Volume and composition of emboli in neuroprotected stenting of the carotid artery. Am. J. Neuroradiol. 30, 473-478.

Poppert H., Wolf O., Resch M., Theiss W., Schmidt-Thieme T., Graefin von Einsiedel H., Heider P., Martinoff S. and Sander D. (2004). Differences in number, size and location of intracranial microembolic lesions after surgical versus endovascular treatment without protection device of carotid artery stenosis. J. Neurol. 251, 1198-1203.

Quan V.H., Huynh R., Seifert P.A., Kuchela A., Chen W.H., Sütsch G., Eisenhauer A.C. and Rogers C. (2005). Morphometric analysis of particulate debris extracted by four different embolic protection devices from coronary arteries, aortocoronary saphenous vein conduits, and carotid arteries. Am. J. Cardiol. 95, 1415-1419.

Rerkasem K., Shearman C.P., Williams J., Morris G.E., Phillips M.J., Calder P.C. and Grimble R.F. (2002). C-reactive protein is elevated in symptomatic compared with asymptomatic patients with carotid artery disease. Eur. J. Vasc. Endovasc. Surg. 23, 505-509.

Roh H.G., Byun H.S., Ryoo J.W., Na D.G., Moon W.J., Lee B.B. and Kim D.I. (2005). Prospective analysis of cerebral infarction after carotid endarterectomy and carotid artery stent placement by using diffusion-weighted imaging. Am. J. Neuroradiol. 26, 376-384.

Ross R. (1999). Atherosclerosis: an inflammatory disease. N. Engl. J. Med. 340, 115-126.

Rost N.S., Wolf P.A., Kase C.S., Kelly-Hayes M., Silbershatz H., Massaro J.M., D'Agostino R.B., Franzblau C. and Wilson P.W. (2001). Plasma concentration of C-reactive protein and risk of ischemic stroke and transient ischemic attack. The framingham study. Stroke 32, 2575-2579.

Schillinger M., Exner M,. Mlekusch W. Sabeti S., Amighi J., Nikowitsch R., Timmel E., Kickinger B., Minar C., Pones M., Lalouschek W., Rumpold H., Maurer G., Wagner O. and Minar E. (2005). Inflammation and carotid artery - Risk for atherosclerosis study (ICARAS). Circulation 111, 2203-2209.

Skjelland M., Krohg-Sørensen K., Tennøe B., Bakke S.J., Brucher R. and Russell D. (2009). Cerebral microemboli and brain injury during carotid artery endarterectomy and stenting. Stroke 40, 230-234.

Tron K., Manolov D.E., Rocker C., Kächele M., Torzewski J. and Nienhaus G.U. (2008). C-reactive protein specifically binds to Fcc receptor type I on a macrophage-like cell line. Eur. J. Immunol. 38, 1414-1422.

Venugopal S.K., Devaraj S. and Jialal l. (2005). Effect of C-reactive protein on vascular cells: evidence for a proinflammatory, proatherogenic role. Curr. Opin. Nephrol. Hypertens. 14, 33-37.